On the Stability of the FDTD Algorithm for Elastic Media at a Material Interface

Christoph T. Schröder, *Student Member, IEEE* and Waymond R. Scott, Jr., *Member, IEEE*

Abstract

In this paper, the stability behavior of the first-order finite-difference time-domain algorithm for elastodynamics at the interface between two different materials is investigated. A necessary condition for stability is established, which, dependent on the material properties of the two media, might be more restrictive than the well-known Courant condition. It is shown that this more restrictive stability condition can be avoided if the material properties are averaged on the boundary.

Keywords

FDTD, finite-difference, elastic, stability

I. Introduction

For many years now, the finite-difference time-domain (FDTD) method has been applied to a wide range of different problems in various fields. Advances in computer technology have made it possible to handle increasingly more complex problems, thus drastically enhancing the versatility and potentiality of the FDTD method. In elastodynamics, the FDTD was introduced in the late 1960's, and due to its accurate results and its algorithmic simplicity it fast gained popularity [1] – [3]. Throughout the years, various elastic finite-difference schemes have been proposed, and the theoretical foundations of the algorithm have been a topic of continuous research ever since.

A significant question that must be considered when applying a numerical algorithm is the question of stability of the algorithm. The stability of difference equations in general and the finite-difference algorithm in particular has been investigated in much detail [4] – [14]. Various aspects of the stability of the FDTD algorithm and its different schemes have been explored, and the mathematical tools to analyze the algorithmic stability are well-established. In this paper, the stability of the first-order finite-difference formulation at an interface between two different materials is investigated.

This work is supported in part under the OSD MURI program by the US Army Research Office under contract DAAH04-96-1-0448 and by a grant from the US Office of Naval Research under contract N00014-99-1-0995.

The authors are with the School of Electrical and Computer Engineering, Georgia Institute of Technology, Atlanta, Ga 30332.

The first-order elastic finite-difference formulation was introduced by Madariaga [15] and Virieux [16], [17]. Contrary to the second-order scheme, which is based on the elastic wave equation, the first-order formulation uses a set of first-order partial differential equations, consisting of the *equation of motion*, the *strain-velocity* relation and the *elastic constitutive relation.* A staggered numerical grid is introduced in which the field components are not known at the same points in space and time. Within the first-order FDTD algorithm, internal boundaries, i. e., boundaries between different materials, are satisfied implicitly. The finite-difference algorithm is usually stable, if the Courant condition is satisfied. However, if media with greatly different material properties are considered, the algorithm turns out to be unstable at the interface and a more restrictive condition for stability arises. In this paper, this stability behavior is analyzed in terms of the difference in material properties between the two adjacent materials. A longitudinal wave normally incident onto a material interface is considered. The matrix method is employed, and a necessary condition for stability is established. It is shown that, if the material parameters are averaged properly on the boundary, the Courant condition poses a necessary condition for stability, and no further restrictions on the stability condition due to the presence of the material interface arise.

To establish the stability condition, some well-known mathematical theorems and procedures are utilized in this paper. The matrix method in conjunction with Gershgorin's Circle theorem has frequently been employed and is well-documented (see [4], [8], [10]). For example, Ilan and Loewenthal used a fairly similar procedure as presented in this paper to analyze the stability of the second-order finite-difference formulation incorporating a free-surface boundary condition [9]. This paper, although similar in its mathematical foundations, explores a quite different aspect by addressing the stability of the first-order scheme at a material interface.

This paper is structured as follows. First, a theoretical analysis is provided which indicates that a more restrictive stability condition arises at a material interface. Second, it is shown that this more restrictive condition can be avoided by averaging the material parameters on the interface. Third, the theoretical results are verified by numerical results. Finally, in an appendix, the averaging procedure is derived and explained.

II. Stability Analysis: Theory

The fundamental condition for stability of the finite-difference algorithm, i. e., the condition that relates the size of the time increment to the spacing of the discrete nodes in the FDTD grid and that must be fulfilled for the finite-difference algorithm to be stable, is the *Courant condition* [18]. The Courant condition states that the physical wave speed of a propagating wave must not exceed the velocity by which information can travel in the discrete grid. Mathematically, for a space step of size Δl, the Courant condition in an n-dimensional grid is

$$\frac{\Delta t}{\Delta l} c_{max} \leq \frac{1}{\sqrt{n}}. \tag{1}$$

Here, Δt denotes the time step, and c_{max} is the maximum wave speed occurring in the solution space. If an infinite homogeneous medium is considered, the Courant condition poses a necessary as well as a sufficient condition for stability [4], [6], [8], [10].

In this section, a necessary condition for stability for the finite-difference algorithm in the presence of an interface between two differing materials is derived. It is shown that this condition might, dependent on the ratio of the two materials, pose a more restrictive condition on stability than the Courant condition. The analysis presented here is performed for a longitudinal wave being normally incident onto a material interface. Results for a transverse wave, however, can be obtained in an analogous way.

A. 1-D Longitudinal Wave Incident onto a Material Interface

The stability behavior of a 1-D finite-difference grid for a longitudinal wave normally incident onto a material interface is to be investigated. The propagation direction coincides with the x-direction, and the only non-zero velocity component is v_x. Figure 1 shows a portion of the discrete first-order finite-difference grid. The material interface is located between T_{xx} at $i - 0.5$ and v_x at i. The first-order finite-difference system of equations can be combined to obtain a second-order formulation in terms of solely the particle velocity. By combining the discrete first-order equations rather than discretizing the second-order wave equation, the stability behavior of the first-order finite-difference formulation is preserved. In the second-order formulation, the stress T_{xx} is eliminated, but the Lamé constants, which are associated with the stress components, are still located half a step in between the velocity components. The second-order finite-difference update equation for the longitudinal particle velocity v_x becomes

$$\begin{aligned} v_x^{k+1}(n) \quad = \quad & v_x^k(n)\left[2 - \frac{\Delta t^2}{\Delta x^2}\frac{\lambda(n-0.5) + 2\mu(n-0.5) + \lambda(n+0.5) + 2\mu(n+0.5)}{\rho(n)}\right] \\ & + v_x^k(n+1)\left[\frac{\Delta t^2}{\Delta x^2}\frac{\lambda(n+0.5) + 2\mu(n+0.5)}{\rho(n)}\right] \\ & + v_x^k(n-1)\left[\frac{\Delta t^2}{\Delta x^2}\frac{\lambda(n-0.5) + 2\mu(n-0.5)}{\rho(n)}\right] \\ & - v_x^{k-1}(n), \end{aligned} \tag{2}$$

where $n = 1 \ldots N$ are the nodes of the 1-D grid and k represents the discrete time step. Again, note that the Lamé constants are placed at the half steps in between the velocity nodes.

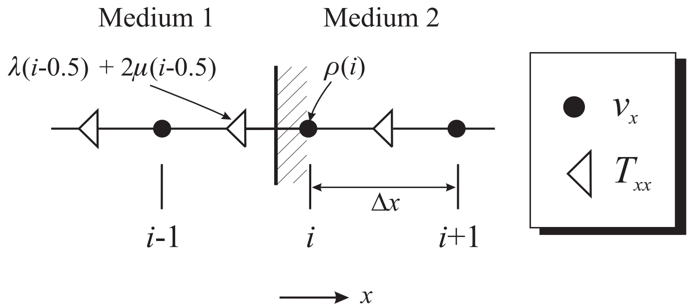

Fig. 1. 1-D finite-difference grid for a longitudinal wave normally incident onto a material boundary.

For a finite-sized problem, the finite-difference scheme can be formulated as a matrix equation [8]. Considering a one-dimensional grid with nodes $n = 1 \ldots N$, and assuming $v_x(0) = v_x(N+1) = 0$ on the outer grid edges at all times, the finite-difference scheme can be written as

$$\mathbf{v_x}^{k+1} = \mathbf{A} \cdot \mathbf{v_x}^{k} - \mathbf{I} \cdot \mathbf{v_x}^{k-1}, \tag{3}$$

where

$$\mathbf{v_x}^{k} = \begin{bmatrix} v_x^k(1) \\ \vdots \\ v_x^k(N) \end{bmatrix}$$

is a vector containing the velocity values at the N nodes at time k, and $\mathbf{I}$ is the $N \times N$ identity matrix. $\mathbf{A}$ is a tri-diagonal matrix:

$$\mathbf{A} = \begin{bmatrix} \ddots & \ddots & & & & & \\ \ddots & 2 - 2\frac{\Delta t^2}{\Delta x^2}c_1^2 & \frac{\Delta t^2}{\Delta x^2}c_1^2 & & & 0 & \\ & \frac{\Delta t^2}{\Delta x^2}c_1^2 & 2 - 2\frac{\Delta t^2}{\Delta x^2}c_1^2 & \frac{\Delta t^2}{\Delta x^2}c_1^2 & & & \\ & & \frac{\Delta t^2}{\Delta x^2}\frac{\lambda_1+2\mu_1}{\rho_2} & 2 - \frac{\Delta t^2}{\Delta x^2}\left(c_2^2 + \frac{\lambda_1+2\mu_1}{\rho_2}\right) & \frac{\Delta t^2}{\Delta x^2}c_2^2 & & \\ & & & \frac{\Delta t^2}{\Delta x^2}c_2^2 & 2 - 2\frac{\Delta t^2}{\Delta x^2}c_2^2 & \frac{\Delta t^2}{\Delta x^2}c_2^2 & \\ & 0 & & & \frac{\Delta t^2}{\Delta x^2}c_2^2 & 2 - 2\frac{\Delta t^2}{\Delta x^2}c_2^2 & \ddots \\ & & & & & \ddots & \ddots \end{bmatrix}, \tag{4}$$

where

$$c_1 = \sqrt{\frac{\lambda_1 + 2\mu_1}{\rho_1}}, \quad c_2 = \sqrt{\frac{\lambda_2 + 2\mu_2}{\rho_2}} \tag{5}$$

describe the longitudinal wave speeds in Medium 1 and Medium 2, respectively. In this matrix, rows $n = 1 \ldots i-1$ describe Medium 1, the i-th row is the material interface, and the rows $n = i+1 \ldots N$

represent Medium 2. Eq. (3) can be written in a more compact form:

$$\begin{bmatrix} \mathbf{v_x}^{k+1} \\ \mathbf{v_x}^{k} \end{bmatrix} = \mathbf{B} \cdot \begin{bmatrix} \mathbf{v_x}^{k} \\ \mathbf{v_x}^{k-1} \end{bmatrix} = \begin{bmatrix} \mathbf{A} & -\mathbf{I} \\ \mathbf{I} & \mathbf{0} \end{bmatrix} \cdot \begin{bmatrix} \mathbf{v_x}^{k} \\ \mathbf{v_x}^{k-1} \end{bmatrix}, \tag{6}$$

where each submatrix of $\mathbf{B}$ is $N \times N$ and, consequently, $\mathbf{B}$ is $2N \times 2N$.

For the finite-difference algorithm to be stable, the magnitude of all eigenvalues of $\mathbf{B}$ must be smaller than or equal to one [4], [8], [10]. However, the eigenvalues cannot be easily determined in closed form and, thus, they are estimated and a necessary condition for stability is established.

The analysis of the eigenvalues is made considerably easier considering the structure of the matrix $\mathbf{B}$. $\mathbf{B}$ consists of four blocks of size $N \times N$: $\mathbf{A}$, $\mathbf{I}$, $-\mathbf{I}$ and $\mathbf{0}$. If a matrix can be divided into $M \times M$ square sub-blocks of equal size $N \times N$, and the sub-blocks have a common set of N linearly independent eigenvectors, then the eigenvalues of the entire matrix are given by the eigenvalues of the matrices

$$\begin{bmatrix} \lambda_{11}^{p} & \cdots & \lambda_{1M}^{p} \\ \vdots & & \vdots \\ \\ \lambda_{M1}^{p} & \cdots & \lambda_{MM}^{p} \end{bmatrix}, \qquad p = 1 \ldots N \tag{7}$$

where p indicates the p-th eigenvector to each sub-block [8].

Since any vector is an eigenvector of $\mathbf{I}$ and $\mathbf{0}$, the four sub-blocks of $\mathbf{B}$ indeed have a common set of eigenvectors: all eigenvectors of $\mathbf{A}$ are also eigenvectors to the identity matrix as well as the zero matrix. The identity matrix has the N-fold eigenvalue one and the zero-matrix has the N-fold eigenvalue zero. Thus, letting λ_{A} indicate any eigenvalue of $\mathbf{A}$, the eigenvalues of $\mathbf{B}$ are given by the eigenvalues of the matrix

$$\begin{bmatrix} \lambda_{\mathrm{A}} & -1 \\ 1 & 0 \end{bmatrix}, \tag{8}$$

and are determined from the quadratic equation

$$1 - \lambda(\lambda_{\mathrm{A}} - \lambda) = 0. \tag{9}$$

The eigenvalues are then

$$\lambda = \frac{\lambda_{\mathrm{A}}}{2} \pm \sqrt{\frac{\lambda_{\mathrm{A}}^{2}}{4} - 1}. \tag{10}$$

Note here that all eigenvalues of $\mathbf{A}$ are real.[1]

[1] A tridiagonal matrix with either all its off-diagonal elements positive or all its off-diagonal elements negative is diagonizable and has only real eigenvalues [8].

The magnitude of all eigenvalues of $\mathbf{B}$ must be smaller than or equal to one: $|\lambda| \leq 1$. For this to be true, it can be shown from Eq. (10) that the magnitude of all eigenvalues of $\mathbf{A}$ must be smaller than or equal to two:

$$|\lambda_{\mathrm{A}}| \leq 2. \tag{11}$$

It is then sufficient to find or estimate the eigenvalues of $\mathbf{A}$ and conclude the stability condition from these.

The eigenvalues of a matrix can most easily be approximated using *Gershgorin's Circle Theorem* [4], [8], [9], [19]. Gershgorin's Circle theorem states that the eigenvalues of a matrix lie within circles in the complex plane whose centers are the elements of the matrix's main diagonal and whose radii are equal to the sum of the magnitude of the off-diagonal row elements:

$$|\lambda_n - a_{nn}| \leq \sum_{\substack{m \\ n \neq m}} |a_{nm}|. \tag{12}$$

From Gershgorin's Theorem it is seen that the eigenvalues of $\mathbf{A}$ lie within three circles:

$$\left|\lambda_{\mathrm{A}} - \left(2 - 2\frac{\Delta t^2}{\Delta x^2} c_1^2\right)\right| \leq 2\frac{\Delta t^2}{\Delta x^2} c_1^2; \tag{13}$$

$$\left|\lambda_{\mathrm{A}} - \left(2 - \frac{\Delta t^2}{\Delta x^2}\left(c_2^2 + \frac{\lambda_1 + 2\mu_1}{\rho_2}\right)\right)\right| \leq \frac{\Delta t^2}{\Delta x^2}\left(c_2^2 + \frac{\lambda_1 + 2\mu_1}{\rho_2}\right); \tag{14}$$

$$\left|\lambda_{\mathrm{A}} - \left(2 - 2\frac{\Delta t^2}{\Delta x^2} c_2^2\right)\right| \leq 2\frac{\Delta t^2}{\Delta x^2} c_2^2. \tag{15}$$

Eq. (13) and Eq. (15) yield the Courant condition for Medium 1 and 2, respectively. Because all eigenvalues of $\mathbf{A}$ are real, λ_{A} according to Eq. (13) will lie in the range

$$2 - 4\frac{\Delta t^2}{\Delta x^2} c_1^2 \leq \lambda_{\mathrm{A}} \leq 2. \tag{16}$$

If $|\lambda_{\mathrm{A}}| \leq 2$ is to be satisfied,

$$\frac{\Delta t^2}{\Delta x^2} c_1^2 \leq 1, \tag{17}$$

which is the Courant condition for Medium 1. Similarly, from Eq. (15), the Courant condition for Medium 2 is obtained as

$$\frac{\Delta t^2}{\Delta x^2} c_2^2 \leq 1. \tag{18}$$

Eq. (14) describes a necessary condition for stability at the node between Medium 1 and 2. For the boundary node, the eigenvalues lie in the range

$$2 - 2\frac{\Delta t^2}{\Delta x^2}\left(c_2^2 + \frac{\lambda_1 + 2\mu_1}{\rho_2}\right) \leq \lambda_{\mathrm{A}} \leq 2. \tag{19}$$

This yields the stability criterion for the boundary node:

$$\frac{\Delta t^2}{\Delta x^2}\left(c_2^2+\frac{\lambda_1+2\mu_1}{\rho_2}\right)\leq 2. \tag{20}$$

The most restrictive of the three conditions (Eq. (17), (18) and (20)) poses the stability condition for the entire system. Note that the overall stability condition is a *necessary* condition. Numerical experiments, however, indicate that the condition is also sufficient for stability.

Eq. (20) can be written as

$$\frac{\Delta t^2}{\Delta x^2}c_2^2\left(1+\frac{\lambda_1+2\mu_1}{\lambda_2+2\mu_2}\right)=\frac{\Delta t^2}{\Delta x^2}c_1^2\frac{\rho_1}{\rho_2}\left(1+\frac{\lambda_2+2\mu_2}{\lambda_1+2\mu_1}\right)\leq 2. \tag{21}$$

For $c_1 > c_2$, the stability condition at the boundary will be most restrictive, if

$$\frac{\rho_1}{\rho_2}\left(1+\frac{\lambda_2+2\mu_2}{\lambda_1+2\mu_1}\right)>2. \tag{22}$$

On the other hand, for $c_2 > c_1$, the boundary stability criterion is most restrictive, if

$$\left(1+\frac{\lambda_1+2\mu_1}{\lambda_2+2\mu_2}\right)>2. \tag{23}$$

Expressed differently, the material interface does not impose an additional constraint on the stability of the finite-difference scheme, if

$$\sqrt{\frac{\lambda_2+2\mu_2}{\lambda_1+2\mu_1}} \geq 1 \qquad \text{or} \tag{24}$$

$$\sqrt{\frac{\lambda_2+2\mu_2}{\lambda_1+2\mu_1}} \leq \sqrt{2\frac{\rho_2}{\rho_1}-1}. \tag{25}$$

This stability bound is plotted in Fig. 2 as a function of $\sqrt{(\lambda_2+2\mu_2)/(\lambda_1+2\mu_1)}$ and $\sqrt{\rho_2/\rho_1}$. The radial lines in Fig. 2 correspond to lines of constant velocity ratios. In the outer region, indicated by *Courant Region* in Fig. 2, the Courant condition is the limiting condition for stability of the finite-difference algorithm. In the region called *Boundary Region*, the stability condition at the boundary is more restrictive than the Courant condition and poses the decisive condition for stability of the finite-difference algorithm.

The same results as above are also obtained when applying the *von-Neumann* (or *Fourier-Series*) method [8], [10]. The von-Neumann method checks for the local stability at a single node in the finite-difference grid in terms of its surrounding nodes. The stability conditions obtained with the von-Neumann method for Medium 1, Medium 2 and the boundary are equivalent to Eqs. (17), (18) and (20), respectively.

Note that, if the boundary in Fig. 1 is placed in between the velocity at node i and the stress at node $i + 0.5$, the bounds on stability will be exactly the same as depicted in Fig. 2, but the ratios

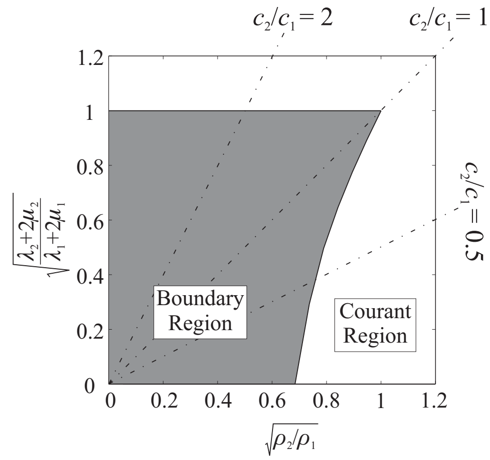

Fig. 2. Stability bounds due to the presence of a material interface.

on the axes are inverted: $\sqrt{\rho_1/\rho_2}$ on the horizontal axis and $\sqrt{(\lambda_1+2\mu_1)/(\lambda_2+2\mu_2)}$ on the vertical axis. Thus, the stability condition at the boundary node now becomes the restrictive condition for stability of the finite-difference algorithm, if the density and the stiffness in Medium 1 are *smaller* than in Medium 2. The analysis of a 1-D shear wave incident onto a material interface is analogous. In fact, by substituting μ_2/μ_1 for $(\lambda_2+2\mu_2)/(\lambda_1+2\mu_1)$ in Eq. (24) and Eq. (25), the bounds for the shear wave case are obtained.

The above description is not very intuitive but rather describes the derivation of a mathematical bound on the stability of the finite-difference algorithm at a boundary. To obtain a more intuitive picture of the actual reason why instabilities occur at the boundary, one can look at the boundary row of $\mathbf{A}$ in Eq. (4). It is seen that in the boundary row a mixed term appears which is composed of the stiffness in Medium 1 and the density in Medium 2: $(\lambda_1+2\mu_1)/\rho_2$. Note that this mixed term has the units of a squared wave speed. Thus, by comparing the value of the mixed term to the wave speeds in the general media, a reason for the instabilities can be suggested. If the longitudinal stiffness in Medium 1 is large or the density in Medium 2 is small (which, for example, is true at the interface between a solid and air), the mixed term might be quite large and, thus, the square root of its value might exceed the wave speeds of Medium 1 and Medium 2. In that case, the stability condition at the boundary can become more restrictive than the Courant condition in the general medium, and neither the Courant condition for Medium 1 nor the one for Medium 2 is a sufficient condition for stability.

B. Averaging the Material Parameters on the Interface

To ensure that the Courant condition is a sufficient condition for stability, the material parameters are averaged for the field components on the boundary. The averaging procedure is briefly described in the Appendix. For the 1-D case discussed above, the velocity component v_x is placed on the boundary (see Fig. 1) and the material density is averaged according to Eq. (37). In the matrix equation (Eq. (4)), only the boundary row of **A** will change, and **A** for the averaged case is obtained by replacing ρ_2 by the averaged density, $(\rho_1 + \rho_2)/2$, throughout the boundary row.

By applying Gershgorin's Circle Theorem to the interface row of the averaged matrix, the eigenvalue associated with this row is determined to lie in the range

$$2 - 2\frac{\Delta t^2}{\Delta x^2}\frac{\lambda_1 + 2\mu_1 + \lambda_2 + 2\mu_2}{(\rho_1 + \rho_2)/2} \leq \lambda_{\mathrm{A}_{avg}} \leq 2. \tag{26}$$

As shown previously, the magnitude of the eigenvalues of **A** must be smaller than two, and the stability condition is obtained as

$$\frac{\Delta t^2}{\Delta x^2}\frac{\lambda_1 + 2\mu_1 + \lambda_2 + 2\mu_2}{\rho_1 + \rho_2} \leq 1. \tag{27}$$

This can be rewritten using the wave speeds as

$$\frac{\Delta t^2}{\Delta x^2}\frac{c_1^2\rho_1 + c_2^2\rho_2}{\rho_1 + \rho_2} = \frac{\Delta t^2}{\Delta x^2}c_1^2\frac{\rho_1 + \rho_2(c_2/c_1)^2}{\rho_1 + \rho_2} = \frac{\Delta t^2}{\Delta x^2}c_2^2\frac{\rho_1(c_1/c_2)^2 + \rho_2}{\rho_1 + \rho_2} \leq 1. \tag{28}$$

When having a closer look at this equation, it becomes clear that the stability condition for the averaged boundary is always less restrictive than the Courant condition in the general medium, and the finite-difference scheme will be stable as long as the Courant condition is satisfied. If $c_1 > c_2$, the stability condition for the entire system is

$$\frac{\Delta t^2}{\Delta x^2}c_1^2 \leq 1, \tag{29}$$

which is the Courant condition for Medium 1. From the second term in Eq. (28), it can be seen that the stability condition for the averaged boundary layer is always less restrictive than the Courant condition for Medium 1, and thus it does not pose any further constraints on the stability of the system. Similarly, if $c_2 > c_1$, the stability condition for the system is

$$\frac{\Delta t^2}{\Delta x^2}c_2^2 \leq 1, \tag{30}$$

which is the Courant condition for Medium 2. From the third term in Eq. (28), it is clear that again the stability criterion for the averaged boundary layer is always satisfied, if the Courant condition for Medium 2 is fulfilled.

C. Numerical eigenvalues of A

Rather than deriving a necessary stability condition by estimating the eigenvalues of **A** using Gershgorin's Circle theorem, the stability condition can also be determined accurately by computing the eigenvalues numerically. For this, the matrix **A** describing the same problem as previously (i. e., a 1-D longitudinal wave and assuming the velocity to be zero on the boundaries) is created and its eigenvalues are determined. A root finder seeks the value of the time step, Δt, for which the magnitude of one or several eigenvalues just exceeds two and, thus, determines the maximum size of the time step that must not be exceeded for the finite-difference algorithm to be stable. The time step is determined for a 1-D grid with 10 nodes.

Fig. 3 shows the necessary stability condition as determined numerically. The stability condition is plotted as a function of the square root of the ratios of the material density and the longitudinal stiffness in the two media. The stability condition is normalized to the value of the time step calculated from the Courant condition in the general medium (Eq. (1)). Due to the normalization, a value of one corresponds to the value predicted by the Courant condition. Values smaller than one represent a condition for stability more restrictive than the Courant condition. In Fig. 3 (a) the material properties are not averaged and in Fig. 3 (b) the material properties are averaged for the velocity component on the interface.

The stability condition derived from the numerically determined eigenvalues verifies the results presented earlier. If the material parameters are not averaged on the material interface, the interface will impose a constraint on the stability condition. If the density ratio $\sqrt{\rho_2/\rho_1}$ and the stiffness ratio $\sqrt{(\lambda_2+2\mu_2)/(\lambda_1+2\mu_1)}$ fall below some critical value (≈ 1), the time step must be chosen smaller than dictated by the Courant condition in order to achieve a stable behavior. When $\sqrt{\rho_2/\rho_1}$ and $\sqrt{(\lambda_2+2\mu_2)/(\lambda_1+2\mu_1)}$ approach zero, the necessary stability condition also approaches zero, and, thus, the required time step becomes infinitely small. For $\sqrt{\rho_2/\rho_1} > 1$ or $\sqrt{(\lambda_2+2\mu_2)/(\lambda_1+2\mu_1)} > 1$, the stability condition at the boundary is less restrictive than the Courant condition. For the averaged case, the boundary does not pose an additional stability constraint, and the Courant condition is the limiting condition for stability independent of the ratios for the material density and Lamé's constants. Similar results have also been obtained for the 2-D first-order formulation.

III. Conclusions

The stability of the first-order FDTD algorithm at a material interface has been analyzed. It has been theoretically shown and verified numerically that the presence of a material interface can pose restrictions on the stability condition of the FDTD algorithm. By averaging the material properties on the interface, the restrictions can be avoided, and the well-known Courant condition will be the limiting condition for stability. A simple averaging procedure is presented in the Appendix. Note that the kind of instabilities described in this paper are not limited to only the first-order FDTD algorithm for elastodynamics. Due to the similarity of the governing equations, the same effects will also be

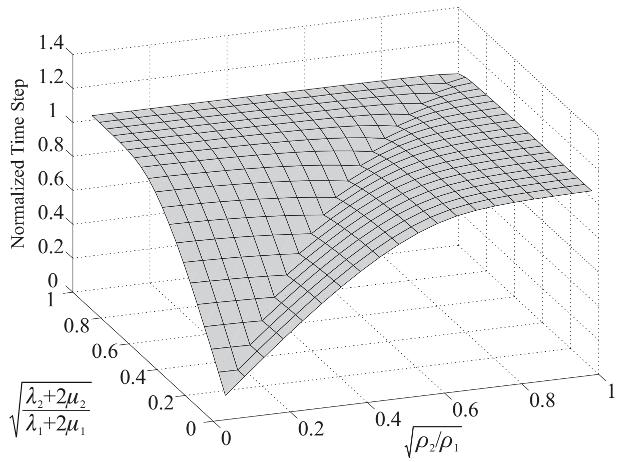

(a)

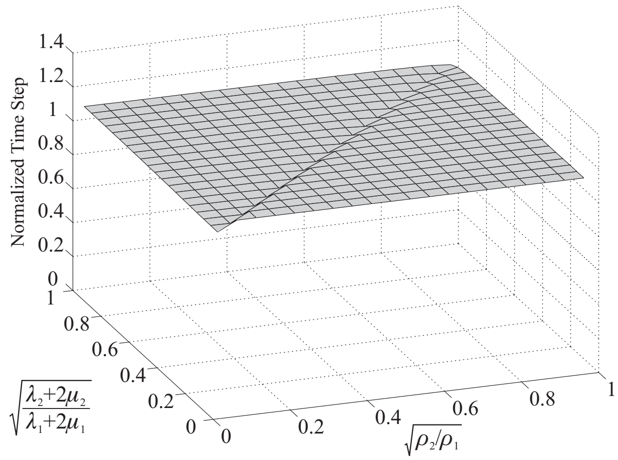

(b)

Fig. 3. Normalized stability condition;(a) material properties not averaged on the boundary, (b) material properties averaged on the boundary.

observed, for example, for the first-order electromagnetic FDTD scheme.

References

[1] Z. Alterman and F. C. Karal, Jr., "Propagation of elastic waves in layered media by finite-difference methods," *Bulletin Seismological Society of America*, vol. 58, no. 1, pp. 367–398, Feb. 1968.

[2] M. Ottaviani, "Elastic wave propagation in two evenly-welded quarter-spaces," *Bulletin Seismological Society of America*, vol. 61, no. 2, pp. 1119–1152, 1971.

[3] K. R. Kelly, R. W. Ward, S. Treitel, and R. M. Alford, "Synthetic seismograms: a finite-difference approach," *Geophysics*, vol. 41, no. 1, pp. 2–27, Feb. 1976.

[4] R. D. Richtmyer and K. W. Morton, *Difference Methods for Initial Value Problems*, John Wiley and Sons, New York, 2$^{\text{nd}}$ edition, 1967.

[5] M. L. Buchanan, "A necessary and sufficient condition for stability of difference schemes for second-order initial value problems," *J. Soc. Indust. Appl. Math.*, vol. 11, no. 2, pp. 474–501, Jun. 1963.

[6] P. Fox, "The solution of hyperbolic partial differential equations by difference methods," in *Mathematical Methods for Digital Computers.* A. Ralston and H.S. Wilf, Editors, Ch. 16, Wiley, New York, 1964.

[7] P. D. Lax and B. Wendroff, "Difference schemes for hyperbolic equations with high order of accuracy," *Comm. Pure Applied Math.*, vol. 17, pp. 381–398, 1964.

[8] G. D. Smith, *Numerical Solution of Partial Differential Equations; Finite Difference Methods*, Clarendon Press, 2^{nd} edition, 1978.

[9] A. Ilan and D. Loewenthal, "Instability of finite difference schemes due to boundary conditions in elastic media," *Geoph. Prosp.*, vol. 24, no. 3, pp. 431–453, Sep. 1976.

[10] A. R. Mitchell and D. F. Griffiths, *The Finite Difference Method in Partial Differential Equations*, John Wiley and Sons, New York, 1980.

[11] B. Kummer and A. Behle, "Second-order finite-difference modeling of SH-wave propagation in laterally inhomogeneous media," *Bulletin Seismological Society of America*, vol. 72, no. 3, pp. 793–808, Jun. 1982.

[12] K. J. Marfurt, "Accuracy of finite-difference and finite-element modeling of the scalar and elastic wave equations," *Geophysics*, vol. 49, no. 5, pp. 533–549, May 1984.

[13] A. Sei, "A family of numerical schemes for the computation of elastic waves," *SIAM J. Scientific Computations*, vol. 16, no. 4, pp. 898–916, Jul. 1995.

[14] J. W. Thomas, *Numerical Partial Differential Equations; Finite Difference Methods*, Springer, 1995.

[15] R. Madariaga, "Dynamics of an expanding circular fault," *Bulletin Seismological Society of America*, vol. 66, pp. 639–666, 1976.

[16] J. Virieux, "SH-wave propagation in heterogenous media: Velocity-stress finite-difference method," *Geophysics*, vol. 49, no. 11, pp. 1933–1957, Nov. 1984.

[17] J. Virieux, "P-SV wave propagation in heterogenous media: Velocity-stress finite-difference method," *Geophysics*, vol. 51, no. 4, pp. 889–901, Apr. 1986.

[18] A. Tavlove, *Computational Electromagnetics: The Finite-Difference Time-Domain Method*, Artech House, Boston, 1995.

[19] D. S. Watkins, *Fundamentals of Matrix Computations*, John Wiley and Sons, New York, 1991.

[20] K. R. Umashankar, A. Tavlove, and B. Beker, "Calculation and experimental validation of induced currents on coupled wires in an arbitrary shaped cavity," *IEEE Trans. Antennas Propagat.*, vol. 35, no. 11, pp. 1248–1257, Nov. 1987.

Appendix

I. Averaging

To ensure the stability of the finite-difference scheme at a material interface, the material parameters are averaged for the field components on the interface. Figure 4 shows a part of a 2-D finite-difference grid including two different media. The boundary between the two media is placed such that the normal particle velocity components are located on the interface. Thus, at a vertical boundary, the velocity component v_x lies on the boundary, whereas v_z is placed on a horizontal boundary. The only stress component that is placed on the boundary is the shear stress T_{xz}. A simple linear averaging procedure is presented which is derived in a straightforward manner from the governing equations in integral form. The derivation is well-known (see, for example, [18], [20]) and is given here for the sake of completeness.

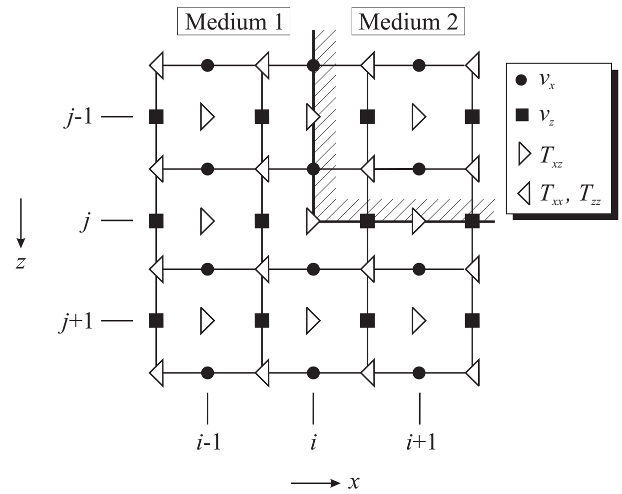

Fig. 4. Boundary between two media in a 2-D finite-difference grid; the normal particle velocities and the shear stress are located on the interface.

A. Material Density

The procedure for averaging the material density on the boundary is derived from the equation of motion. The derivation of the averaging is analogous for both the horizontal and vertical boundary and, thus, the averaging procedure is presented only for the horizontal particle velocity on a vertical interface. The equation of motion,

$$\nabla \cdot \mathbf{T} = \rho \frac{\partial \mathbf{v}}{\partial t}, \tag{31}$$

is expanded for the 2-D Shear-Vertical (S-V) case in the x-z plane:

$$\frac{\partial}{\partial x} T_{xx} + \frac{\partial}{\partial z} T_{xz} = \rho \frac{\partial v_x}{\partial t} \tag{32}$$

$$\frac{\partial}{\partial x} T_{xz} + \frac{\partial}{\partial z} T_{zz} = \rho \frac{\partial v_z}{\partial t}. \tag{33}$$

The only non-zero velocity components are v_x and v_z. Considering the horizontal particle velocity v_x, the procedure for averaging the material density on the vertical boundary is derived by integrating Eq. (32) over a box enclosing a portion of the boundary as depicted in Fig. 5:

$$\iint_{Box} \left[\frac{\partial}{\partial x} T_{xx} + \frac{\partial}{\partial z} T_{xz} \right] dx\, dz = \oint \left(T_{xx} \hat{\mathbf{x}} + T_{xz} \hat{\mathbf{z}} \right) \hat{\mathbf{n}}\, ds = \iint_{Box} \rho \frac{\partial v_x}{\partial t}\, dx\, dz, \tag{34}$$

where the density ρ is a function of position, and Gauss' integral theorem has been applied to convert the surface integral on the left hand side into a contour integral; $\hat{\mathbf{n}}$ is the normal vector to the contour of the area, and $\hat{\mathbf{x}}$ and $\hat{\mathbf{z}}$ are normal vectors in the x- and z-direction, respectively.

Using the discrete finite-difference formulation, the integration is carried out over a box of area $\Delta A = \Delta x \cdot \Delta z$, equivalent to the size of one cell of the finite-difference grid (see Fig. 5). Assuming the

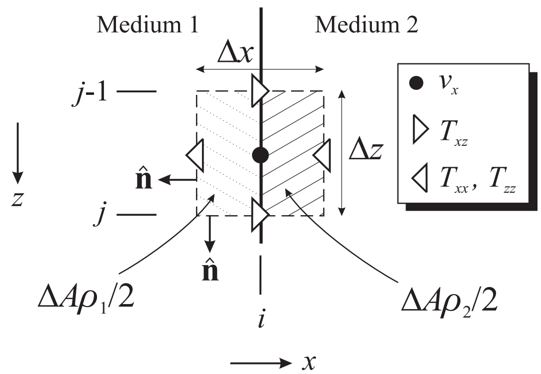

Fig. 5. Averaging of the material density ρ; the normal stress components are integrated along the contour.

boundary between Medium 1 and Medium 2 divides the area of integration in half, the integral comes out to be

$$\frac{\rho_1+\rho_2}{2}\Delta A\cdot\frac{v_x^{k+0.5}(i,j-0.5)-v_x^{k-0.5}(i,j-0.5)}{\Delta t}= \\ \Big(T_{xx}^k(i+0.5,j-0.5)-T_{xx}^k(i-0.5,j-0.5)\Big)\cdot\Delta z+\Big(T_{xz}^k(i,j)-T_{xz}^k(i,j-1)\Big)\cdot\Delta x. \quad (35)$$

After dividing by ΔA, the finite-difference approximation to Eq. (32) is obtained:

$$\frac{\rho_1+\rho_2}{2}\cdot\frac{v_x^{k+0.5}(i,j-0.5)-v_x^{k-0.5}(i,j-0.5)}{\Delta t}= \\ \frac{T_{xx}^k(i+0.5,j-0.5)-T_{xx}^k(i-0.5,j-0.5)}{\Delta x}+\frac{T_{xz}^k(i,j)-T_{xz}^k(i,j-1)}{\Delta z}. \quad (36)$$

Thus, for the velocity components on the boundary, the material densities of the two media are averaged linearly:

$$\rho_{avg}=(\rho_1+\rho_2)/2. \quad (37)$$

The same result is obtained for the vertical particle velocity on a horizontal interface.

B. Lamé's Constants

The procedure for averaging Lamé's constants for the stress components on the boundary is derived by using the elastic constitutive relation together with the strain-velocity relation. The elastic constitutive relation combines the mechanic strain and the stress and is usually expressed as

$$\mathbf{T}=\mathbf{c}\cdot\mathbf{S}, \quad (38)$$

where the stress $\mathbf{T}$ and the strain $\mathbf{S}$ are 3×3 tensors and the stiffness matrix $\mathbf{c}$ is a four-dimensional tensor of size $3\times3\times3\times3$. For an isotropic and lossless medium, the entries of the stiffness matrix are completely described by two independent constants, Lamé's constants λ and μ.

In the 2-D finite-difference gird (Fig. 4), the shear stress T_{xz} is placed on the boundary and, consequently, Lamé's constants are averaged for only T_{xz}. After combining the strain-velocity relation and the constitutive relation, an equation relating v_x and v_z to T_{xz} arises, from which, in the finite-difference formulation, the shear stress is determined:

$$\frac{\partial v_x}{\partial z} + \frac{\partial v_z}{\partial x} = \frac{1}{\mu}\frac{\partial T_{xz}}{\partial t}. \tag{39}$$

The averaging of μ is achieved by integrating over a box enclosing parts of the boundary, and Eq. (39) becomes

$$\iint_{Box} \left[\frac{\partial v_x}{\partial z} + \frac{\partial v_z}{\partial x}\right] dx\, dz = \iint_{Box} \frac{1}{\mu}\frac{\partial T_{xz}}{\partial t}\, dx\, dz. \tag{40}$$

Figure 6 shows the integration contour around T_{xz}. Applying Stoke's integral theorem, the left hand side of Eq. (40) can be written as

$$\iint_{Box} \left[\frac{\partial v_x}{\partial z} + \frac{\partial v_z}{\partial x}\right] dx\, dz = \iint_{Box} \nabla \times (v_x \cdot \hat{\mathbf{x}} - v_z \cdot \hat{\mathbf{z}})\, d\vec{A} = \oint (v_x \cdot \hat{\mathbf{x}} - v_z \cdot \hat{\mathbf{z}})\, d\vec{s}. \tag{41}$$

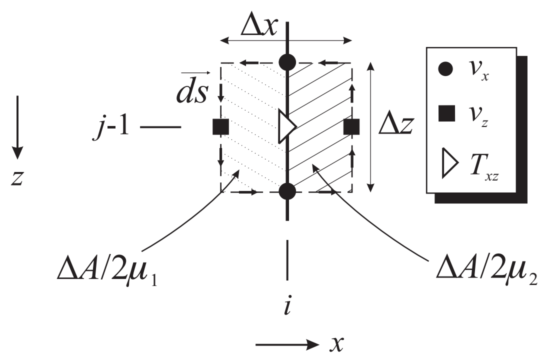

Fig. 6. Averaging of the shear stiffness μ; the tangential velocity components are integrated along the contour.

Using the discrete finite-difference formulation and Eq. (41), Eq. (40) becomes

$$\begin{aligned}&\left(v_x^{k+0.5}(i,j-0.5) - v_x^{k+0.5}(i,j-1.5)\right)\cdot \Delta x + \left(v_z^{k+0.5}(i+0.5,j-1) - v_z^{k+0.5}(i-0.5,j-1)\right)\cdot \Delta z = \\ &\quad \frac{\Delta A}{2}\left(\frac{1}{\mu_1} + \frac{1}{\mu_2}\right)\frac{T_{xz}^{k+1}(i,j-1) - T_{xz}^{k}(i,j-1)}{\Delta t}.\end{aligned} \tag{42}$$

Thus, the inverse of the shear stiffness μ is averaged on the boundary between two media as

$$\frac{1}{\mu_{avg}} = \frac{1}{2}\left(\frac{1}{\mu_1} + \frac{1}{\mu_2}\right). \tag{43}$$

The same is obtained for the field components on a horizontal boundary. For the shear stress on a corner of the boundary (see $T_{xz}(i,j)$ in Fig. 4), the integration yields

$$\frac{1}{\mu_{avg}} = \frac{1}{4}\left(\frac{3}{\mu_1} + \frac{1}{\mu_2}\right). \tag{44}$$